



## City Research Online

### City, University of London Institutional Repository

---

**Citation:** Soysouvanh, S., Phongsanam, P., Mitatha, S., Ali, J., Yupapin, P., Amiri, I. S., Grattan, K. T. V. & Yoshida, M. (2019). Ultrafast all-optical ALU operation using a soliton control within the cascaded InGaAsP/InP microring circuits. *Microsystem Technologies*, 25(2), pp. 431-440. doi: 10.1007/s00542-018-4011-2

This is the accepted version of the paper.

This version of the publication may differ from the final published version.

---

**Permanent repository link:** <https://openaccess.city.ac.uk/id/eprint/20075/>

**Link to published version:** <https://doi.org/10.1007/s00542-018-4011-2>

**Copyright:** City Research Online aims to make research outputs of City, University of London available to a wider audience. Copyright and Moral Rights remain with the author(s) and/or copyright holders. URLs from City Research Online may be freely distributed and linked to.

**Reuse:** Copies of full items can be used for personal research or study, educational, or not-for-profit purposes without prior permission or charge. Provided that the authors, title and full bibliographic details are credited, a hyperlink and/or URL is given for the original metadata page and the content is not changed in any way.

---

City Research Online:

<http://openaccess.city.ac.uk/>

[publications@city.ac.uk](mailto:publications@city.ac.uk)

---

# Ultrafast all-optical ALU operation using a soliton control within the cascaded *GaAsInP/P* microring circuits

S. Soysouvanh<sup>1</sup>, P. Phongsanam<sup>2</sup>, S. Mitatha<sup>1\*</sup>, J. Ali<sup>3</sup>, P. Yupapin<sup>4, 5\*</sup>, I.S. Amiri<sup>6</sup>, K.T.V. Grattan<sup>7</sup>, and M. Yoshida<sup>8</sup>

<sup>1</sup>Department of Computer Engineering, Faculty of Engineering, King Mongkut's Institute of Technology Ladkrabang, Bangkok, 10520, Thailand;

<sup>2</sup>Faculty of Engineering, Kasem Bundit University, 1761 Phatthanakan Rd, Suan Luang, Bangkok 10250, Thailand;

<sup>5</sup>Laser Center, IbnuSina Institute for Industrial and Scientific Research, UniversitiTeknologi Malaysia (UTM);

<sup>4</sup>Computational Optics Research Group, Advanced Institute of Materials Science, Ton Duc Thang University, District 7, Ho Chi Minh City, 700,000, Vietnam;

<sup>5</sup>Faculty of Electrical & Electronics Engineering; Ton Duc Thang University, District 7, Ho Chi Minh City, 700,000, Vietnam;

<sup>6</sup>Division of Materials Science and Engineering, Boston University, Boston, MA, 02215, USA;

<sup>7</sup>Department of Electrical & Electronic Engineering, School of Mathematics, Computer Science & Engineering, The City, University of London, EC1V 0HB, United Kingdom;

<sup>8</sup>Department of Embedded Technology, School of Information and Telecommunication Engineering, Tokai University, 2-3-23, Takanawa, Minato-ku, Tokyo, 108-8619, Japan;

\*Corresponding author E-mails: [kmsomsak@kmitl.ac.th](mailto:kmsomsak@kmitl.ac.th), [preecha.yupapin@tdt.edu.vn](mailto:preecha.yupapin@tdt.edu.vn)

**Abstract:** A dark-bright soliton conversion is used to perform the two arithmetic logic unit (ALU) operations namely adder and subtractor operations. The advantage of the system such as power stability, non-dispersion and the dark-bright soliton phase conversion control can be obtained. The input source into the circuit is the bright soliton pulse, with the pulse width of 35 ps, the peak power at 1.55  $\mu\text{m}$  is 1 mW. By using the dark-bright soliton conversion pair, the generated logic bits can be controlled, and the secure bits can be achieved. The simulation results show the output signal with a minimum loss of only 0.1% with respect to a low input power of 1 mW, and ultra-fast response time of about 0.30 ps can be achieved. It gives the ultra-high bandwidth of more than 40 Gbits<sup>-1</sup>. The circuit composes 6 microring resonators made of *InGaAsP/InP* material with smaller ring radii of 1.5  $\mu\text{m}$ , and the total physical scale of the circuit less than 100  $\mu\text{m}^2$ .

**Keywords:** Ultrafast ALU; All-optical ALU; Microring circuit; GaAsInP/P circuit; Soliton conversion

## 1. Introduction

By reason of the rapid improvements in optical or photonic computing for higher computation, processing speeds and minimal transmission losses are desirable. For decades, most research and investigation is on replacing current computer component redundancy with the equipment, resulting in the optical digital computing systems for processing optical binary data [1-4]. All-optical adders are important elements in any all-optical arithmetic and logical units, many researchers have demonstrated various techniques to perform all-optical arithmetic and logical operations [5-10]. Furthermore, the increasing demand on miniaturizing quantum computers requires an improvement in power consumption. However, most of the previous works need the use of optoelectronic devices in which 30% loss in electro-optic conversion is observed in addition to the decrease in transmission speed. However, such problems are overcome by the use of another form of the input data source, which is known as the optical soliton pulse [11-12] propagating within nonlinear material i.e., *InGaAsP/InP* [13]. It can provide optical-electrical-optical (OEO) conversions, thus lessening the need for electrical power and reduce the transmission loss. This paper presents a 1-bit all-optical full-adder and subtractor circuit which can be used to design 1-bit all-optical arithmetic unit (AU) to perform 4 arithmetic operations i.e. addition, subtraction, increment and decrement based on microring resonator device with a scale of 1.5  $\mu\text{m}$  radius [14], which has been fabricated and demonstrated in various applications [15-19]. The design circuit can offer the advantage of dark-bright soliton conversion control technique within the ring resonator [20-21], in which the optical logic "0" and logic "1" are represented by optical dark soliton "D" and bright soliton "B" pulses, respectively. In this paper, the advantage of the dark-bright soliton conversion signal is employed, from which the generated codes can be used for security purpose. In addition, the ultrafast switching of the soliton pulse property can speed up the process of code generation. The combination of the bit operation is obtained by the cascaded mirroring circuits, which are six *GaAsInP/P* microring devices in the design. Simulations show that the proposed full-adder and full subtractor achieved high-speed operation with and small time-delay compared to other 1-bit conventional adders [22-23], and the experimental results of ring resonator [24] show high-quality factors (Q), free spectral range (FSR), obtainable from ring resonator.

## 2. Operating Principle

An arithmetic unit (AU) is a combinational circuit integrated into an arithmetic logic unit (ALU) that performs arithmetic operations on integer binary numbers. This is in contrast to an (FPU), which operates on floating point numbers. An AU is a fundamental building block of many types of computing circuits, including the central processing unit (CPU) of computers, the floating-point unit (FPUs), and graphics processing units (GPUs). A single CPU, FPU or GPU may contain multiple ALUs. The addition and subtraction are the basis for many important operations such as address generation, multiplication, division which are commonly used in ALUs. In the 1-bit arithmetic unit with two selected inputs can perform 4 arithmetic operations such as addition, subtraction, increment and decrement based on a full-adder circuit. Several designs of adders have been proposed. In [22], all-optical half-adder using Terahertz optical asymmetric demultiplexer (TOAD) switch is proposed. The proposed model is attractive since no additional input beam is used in a half-adder unit and also the numerical simulation is done at 11.11 Gbps in order to investigate the suitable operating condition. However, due to their slow processing speed is quite low compared to other state-of-art designs. In [23], the authors show a new and potentially integrable scheme for the realization of an all-optical binary full adder, using a Mach-Zehnder interferometer (MZI) based on a semiconductor optical amplifier (SOA). The designed system has a successful operation of at 10 Gb/s with return-to-zero modulated signals. But due to a lot of circuit elements may result in the large physical size of the full adder, which inhibits integration. Therefore, in this paper present the new technique that can implement the logic operation with ultra-fast switching time, and can reduce the physical size of the overall system, which is useful for further photonic integration. In our previous work [15] shows the illustration of the dark-bright soliton conversion signal that can form an all-optical half-adder which is very simple and flexible system. In operation, an optical channel dropping filter (OCDF) based microring resonator (MRR) is made up of two straight waveguides coupled with a ring-type waveguide, which is given in the following section. Here Fig. 1 (a) is represented by Fig. 1 (b) for consistency.

The coupling equation outlined in the reference [25, 26] demonstrates a relative phase of between the input signal at the input port and the signal coupled into the ring. Likewise, the signal coupled into the drop and through ports, where both are acquired a phase of  $\pi/2$  regarding the signal in the input port. From Fig. 2, we can obtain the electrical fields of MRR as following equations.

$$E_{ra} = -j\kappa_1 E_{in} + \tau_1 E_{rb} \exp\left(\frac{j\omega T}{2}\right) \exp\left(\frac{-\alpha L}{4}\right) \quad (1)$$

$$E_{rb} = j\kappa_2 E_{ad} + \tau_2 E_{ra} \exp\left(\frac{j\omega T}{2}\right) \exp\left(\frac{-\alpha L}{4}\right) \quad (2)$$

$$E_{th} = \tau_1 E_{in} - j\kappa_1 E_{rb} \exp\left(\frac{j\omega T}{2}\right) \exp\left(\frac{-\alpha L}{4}\right) \quad (3)$$

$$E_{dr} = \tau_2 E_{ad} - j\kappa_2 E_{ra} \exp\left(\frac{j\omega T}{2}\right) \exp\left(\frac{-\alpha L}{4}\right) \quad (4)$$

Where  $E_{in}$  is the input electric field,  $E_{ad}$  is the add (control) electric field,  $E_{th}$  is the output electric field at through port,  $E_{dr}$  is the output electric field at drop port,  $E_{ra}$  and  $E_{rb}$  are the electric fields circulating inside the ring at point  $a$  and  $b$ , respectively.  $\kappa_1$  is the field coupling coefficient between the input and the ring,  $\kappa_2$  is the field coupling coefficient between the ring and the output bus,  $L$  is the circumference of the ring ( $L = 2\pi R$ ), here  $R$  is the radius of the ring measured from the center of the ring to the center of the waveguide.  $T$  is the field propagation time taken for one roundtrip inside the ring ( $T = Ln_{eff}/c$ ), and  $\alpha$  is the power loss in the ring per unit length. We assume that lossless coupling, i.e.  $\tau_{1,2} = \sqrt{1 - \kappa_{1,2}^2}$ . The transfer function of output power/intensities at through port and drop port is given by (5) and (6), respectively.

$$|E_{th}|^2 = \left| \frac{\tau_2 - \tau_1 A \Phi}{1 - \tau_1 \tau_2 A \Phi} E_{in} + \frac{-\kappa_1 \kappa_2 A_{1/2} \Phi_{1/2}}{1 - \tau_1 \tau_2 A \Phi} E_{ad} \right|^2 \quad (5)$$

$$|E_{dr}|^2 = \left| \frac{\tau_2 - \tau_1 A \Phi}{1 - \tau_1 \tau_2 A \Phi} E_{ad} + \frac{-\kappa_1 \kappa_2 A_{1/2} \Phi_{1/2}}{1 - \tau_1 \tau_2 A \Phi} E_{in} \right|^2 \quad (6)$$

Where  $A_{1/2} = \exp(-\alpha L/4)$  is the half-roundtrip amplitude ( $A = A_{1/2}^2$ ),  $\Phi_{1/2} = \exp(j\omega T/2)$  is the half-roundtrip phase contribution ( $\Phi = \Phi_{1/2}^2$ ).  $\tau_{1,2} = \sqrt{1 - \kappa_{1,2}^2}$ ,  $\kappa_1$  and  $\kappa_2$  are the coupling constants.

The input and control electric fields at the input port and drop port are formed by optical dark soliton ( $E_{in(D)}$ ) and bright soliton ( $E_{in(B)}$ ) as given in (7) and (8), respectively.

$$E_{in(D)}(t) = A_0 \tanh\left[\frac{T}{T_0}\right] \exp\left[\left(\frac{z}{2L_D}\right) - i\omega_0 t\right] \quad (7)$$

$$E_{in(B)}(t) = A_0 \operatorname{sech}\left[\frac{T}{T_0}\right] \exp\left[\left(\frac{z}{2L_D}\right) - i\omega_0 t\right] \quad (8)$$

Where  $A$  is the optical field amplitude and  $z$  is the propagation distance.  $T$  is the soliton propagation time in the frame moving at the group velocity ( $T = t - \beta_1 z$ ), here  $\beta_1$  and  $\beta_2$  are the coefficients of the linear and second-order terms of Taylor expansion of the propagation constant.  $L_d$  is the dispersion length of the soliton pulse ( $L_d = T_0^2 / |\beta|$ ).  $T_0$  is the initial soliton pulse width, where  $t$  is the soliton phase shift time, and  $\omega_0$  is the frequency of the soliton.

The above solutions describe a pulse that keeps its temporal width invariance as it propagates and thus is called a temporal soliton. When a soliton peak intensity is ( $\beta/\Gamma T_0^2$ ), then  $T_0$  is known. In case of the soliton pulse in the micro (or nano) ring device is applied, a balance length should be achieved between dispersion length ( $L_d$ ), where the nonlinear length is ( $L_{nl} = 1/\Gamma\phi_{nl}$ ), where  $\Gamma$  is the length scale over which dispersive or nonlinear effects make the beam become wider or narrower ( $\Gamma = n_2 k_0$ ). There is a balance between dispersion and nonlinear lengths, hence,  $L_d = L_{nl}$ . When light propagates within the nonlinear material (medium), the refractive index ( $n$ ) of light within the medium is given by  $n = n_0 + n_2 I = n_0 + n_2 (P/A_{eff})$ , where  $n_0$  and  $n_2$  are the linear and nonlinear refractive indexes, respectively.  $I$  is the optical intensity and  $P$  is the optical power.  $A_{eff}$  is the effective mode core area of the device. For micro/nano ring resonator, the effective mode core areas range from 0.1 to 0.5  $\mu m^2$  [15]. The resonant output of the light field is the ratio between the output field ( $E_{out}(t)$ ) and input field ( $E_{in}(t)$ ) in each roundtrip.

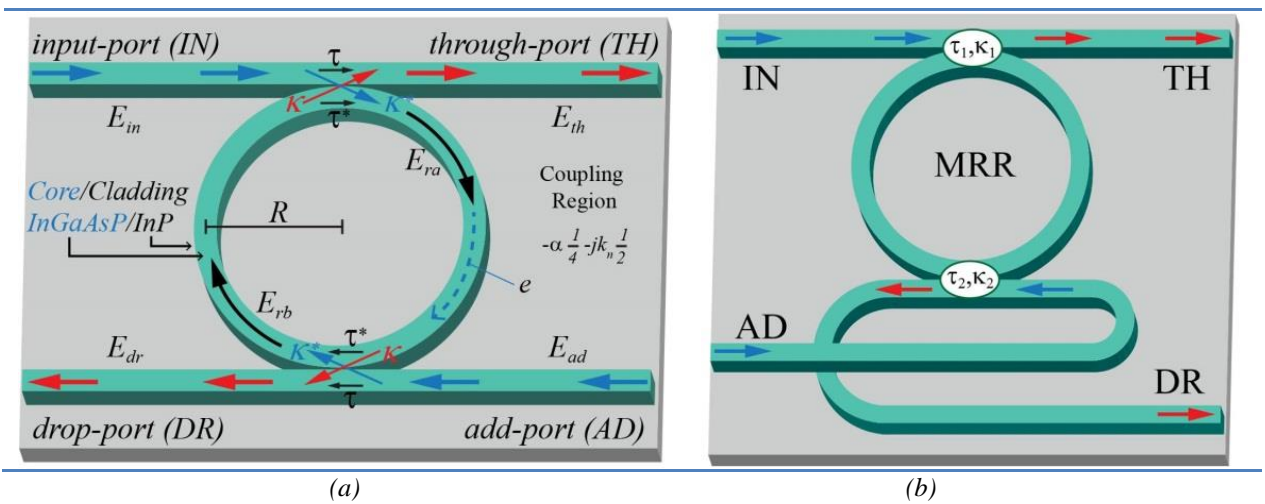


**Fig. 1:** A schematic of a micro-ring resonator (MRR) system, where  $E_{in}$ ,  $E_{th}$ ,  $E_{dr}$  and  $E_{add}$  are the optical field at the input, through and drop ports, respectively. IN, TH, DR and AD are the microring circuit at the input, through and drop ports, respectively.

### 3. Design of All-optical ALU

In order to design the all-optical circuit of the arithmetic logic unit (ALU) for operating two arithmetic operations i.e., full-addition (FA) and full-subtraction (FS) with three binary inputs (XYZ), we relied on the truth table of binary arithmetic operation as illustrated in Table 1, where we can get simplified Boolean's equations obtained as a sum of product for each output as shown in Table 1, we can design an ALU circuit for performing FA and FS by combining the summation of FA (*Sum*) and difference of FS (*Diff*) together as illustrated in Fig. 2. In the design, a circuit consists of 6 microring resonator (MRRs), 5 beam splitters (B.S.) and 5 beam combiners (B.C.). Here the approximate physical size of the MRR is 6  $\mu\text{m}$  wide, 8  $\mu\text{m}$  long, 250 nm thick, has 290-440 nm of waveguide width and  $\sim 1.5 \mu\text{m}$  of ring radius [14]. The proposed scheme of all-optical ALU is shown in Fig. 2. Initially when the input pulse train and control pulse is input into the first microring (MRR1) using dark soliton (logic 0) or bright soliton (logic 1), then the optical soliton is converted to be dark and bright via MRR1 which can be seen at the through port and drop port with  $\pi$  phase shift [28], and MRR1 then functions as an inverter gate like. Hence, the outputs of MRR1 can be written as  $TH1 = \bar{X}$  and  $DR1 = X$ . Subsequently, the output signals from MRR1 are applied into input-ports of MRR2 and MRR3. Next, the input data "Y" with logic "0" (Dark) or logic "1" (Bright) are added into both add-ports and then the dark-bright soliton conversion with  $\pi$  phase shift is operated again by using MRR2 and MRR3. The results obtained are simultaneously seen at the output ports of MRR2 and MRR3 for optical logic operation and can be written as  $TH2 = \bar{X}Y$ ,  $DR2 = \bar{X}\bar{Y}$ ,  $TH3 = XY$ ,  $DR3 = X\bar{Y}$  which can be used to perform half-addition (HA) and half-subtraction (HS) as  $S_{HA} = D_{HS} = \bar{X}Y + X\bar{Y}$ ,  $C_{HA} = XY$ , and  $B_{HS} = \bar{X}\bar{Y}$ . To operate the all-optical HA and HS [15] can be easily done by using beam splitters (B.S) and beam combiners (B.C) e.g., a fiber coupler or optical Y-branch. The beam splitters used in the system are not polarizing. The ratio of reflection-transmission is 50:50 (or 50%) for all polarizations of the incident light. Then the operation of full-adder (FA) and full-subtractor (FS) can be performed by using MRR4, both input signals are generated by the first HA state ( $S_{HA}$ ), then the dark-bright soliton conversion is operated again and generate the output at output-port  $TH4 = S_{HA}$ ,  $DR4 = \bar{S}_{HA}$ . Both output signals are applied to be the input signals of MRR5 and MRR6, respectively. This state, an optical input pulse "Z" with logic "0" or logic "1" is input into both add-ports (MRR5 and MRR6) then the last operation of dark-bright conversion is done again by MRR5 and MRR6. The results are obtained simultaneously at output-ports as  $TH5 = \bar{S}_{HA}Z$ ,  $DR5 = S_{HA}\bar{Z}$ ,  $TH6 = S_{HA}Z$  and  $DR6 = S_{HA}\bar{Z}$ .

**Table 1** – Truth table of binary arithmetic operation

Inputs			Addition		Subtraction	
X	Y	Z	Sum	Carry	Diff	Borrow
0	0	0	0	0	0	0
0	0	1	1	0	1	1
0	1	0	1	0	1	1
0	1	1	0	1	0	1
1	0	0	1	0	1	0
1	0	1	0	1	0	0
1	1	0	0	1	0	0
1	1	1	1	1	1	1

Finally, the full-addition/subtraction is done by combining the optical signal from output-ports of MRR2, MRR3, MRR5 and MRR6, where the full-addition and full-subtraction are expressed by equations (9) – (12).

$$Sum = \bar{S}_{HA}Z + S_{HA}\bar{Z} = TH5 + DR6 \quad (9)$$

$$Carry = XY + S_{HA}Z = TH3 + TH6 \quad (10)$$

$$\text{Difference} = \overline{D_{HS}}Z + D_{HS}\overline{Z} = TH5 + DR6 \quad (11)$$

$$\text{Borrow} = \overline{XY} + S_{HA}Z = TH2 + TH5 \quad (12)$$

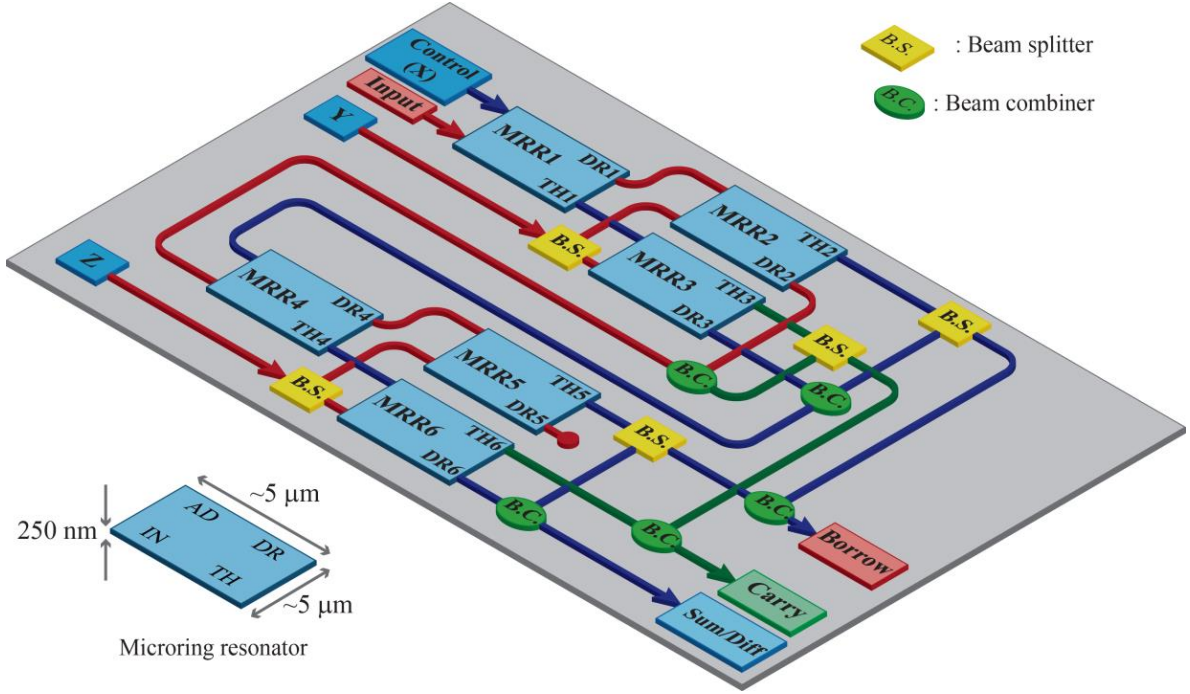


**Fig. 2.** A schematic of the designed circuit for all-optical ALU circuit, where Y and Z: the input soliton pulse, MRR: Microring circuit, IN, TH, DR and AD are the microring circuit at the input, through, drop and add ports, respectively.

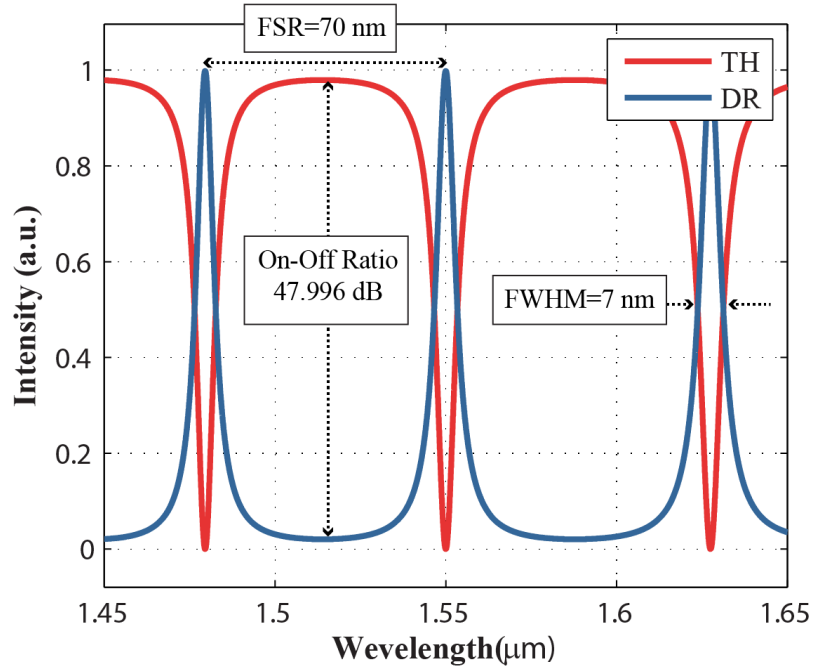
#### 4. Simulation Results and Discussion

In a simulation, in order to perform optical switch with an optimum result, the parameters are fixed for all MRR as shown in Table 2. The input power for dark and bright soliton pulses is 1 mW, soliton pulses width is 35 ps and the center wavelength is  $\lambda_0=1.55 \mu\text{m}$ , and the ring radius is  $1.55 \mu\text{m}$ . The transmission characteristic of MRR is as shown in Fig. 5, where the on-off ratio is 47.99 dB, the free spectral range (FSR) is 70 nm, and the full-width at half maximum (FWHM) is 7 nm. The suitable parameters used in our simulation are concluded in Table 2. Based on nonlinear optical effect cross-phase modulation (XPM) is applied in this mechanism in order to reduce or change the refractive index of MRR. The optical signals at through-port and drop-port can be controlled, which can perform the optical switching in InGaAsP/InP material based [28], and represented the logic NOT gate as illustrated in Fig. 4. The optical logic switching can be concluded that, when there is no control signal (the signal at add-port), the input signal will be transmitted to drop-port (DR). In another side, when the control signal is applied, then the refractive index of the waveguide is changed and causes the change of resonant wavelength, thus the input signal will be transmitted to through-port (TH). The operations of all-optical simultaneous full adder/subtractor are concluded in Table 3 and Fig. 5. Fig. 5(a) shows the transmitted signal at output-ports of ALU circuit for the first case where control input “XYZ” is “000”. Initially, the continuous input signal is input into MRR1 via the input port and there is no control signal ( $X=0$ ), hence the optical signal is transmitted drop-port (DR1) due to resonance condition. Subsequently, the optical signal from DR1 is input into MRR2 via an input port and there is no control input ( $Y=0$ ) is applied to MRR2, therefore, the optical signal will be appeared at drop-port (DR2) to be optical logic “1”. The optical signal from DR2 is then used to be input signal of MRR4 via input-port and appear at the drop-port (DR4) due to the resonance condition. The signal is then input into input-port of MRR5 and then no control input ( $Z=0$ ) is applied to MRR5, hence, the optical signal is again transmitted to drop-port (DR5) due to resonance condition and represents the optical logic “01000100” at output-ports “TH2-DR2-TH3-DR3-TH5-DR5-TH6-DR6”, respectively. Fig. 5(b) shows the transmitted signal when the input XYZ is “001”, for in this case

at the initial state is the same as the previous case where control input ( $XY=00$ ). Therefore, the input signal is transmitted to drop-ports (DR2 and DR4) and later on input into MRR5 via input-port. For this state, the control input is applied ( $Z=1$ ), thus, the optical signal is switched from drop-port (DR5) to through-port (TH5) and represents the optical logic “01001000” at output-ports “TH2-DR2-TH3-DR3-TH5-DR5-TH6-DR6”. Fig. 5(c) shows the output signal when the input XYZ is “010”. This case, there is no control input ( $X=0$ ) is applied to MRR1, thus the input signal is transmitted into drop-port (DR1) again. Next, the signal from DR1 is input into MRR2 via input-port and control input ( $Y=1$ ) is applied to MRR2 via add-port, therefore, the optical signal is switched from drop-port (DR2) to through-port (TH2) as optical logic “1”. The signal from TH2 is later on used as the input signal of MRR4 via add-port and appear at the through-port (TH4) due to the resonance condition, and then applied to MRR6 via input-port. For this state, control input ( $Z=1$ ) is applied to MRR6 via add-port, thus, the optical signal is transmitted to drop-port (DR6) and represents the optical logic “10000001” at output-ports “TH2-DR2-TH3-DR3-TH5-DR5-TH6-DR6”.

Table 2: Ring resonator parameters used in simulation for optimum outputs

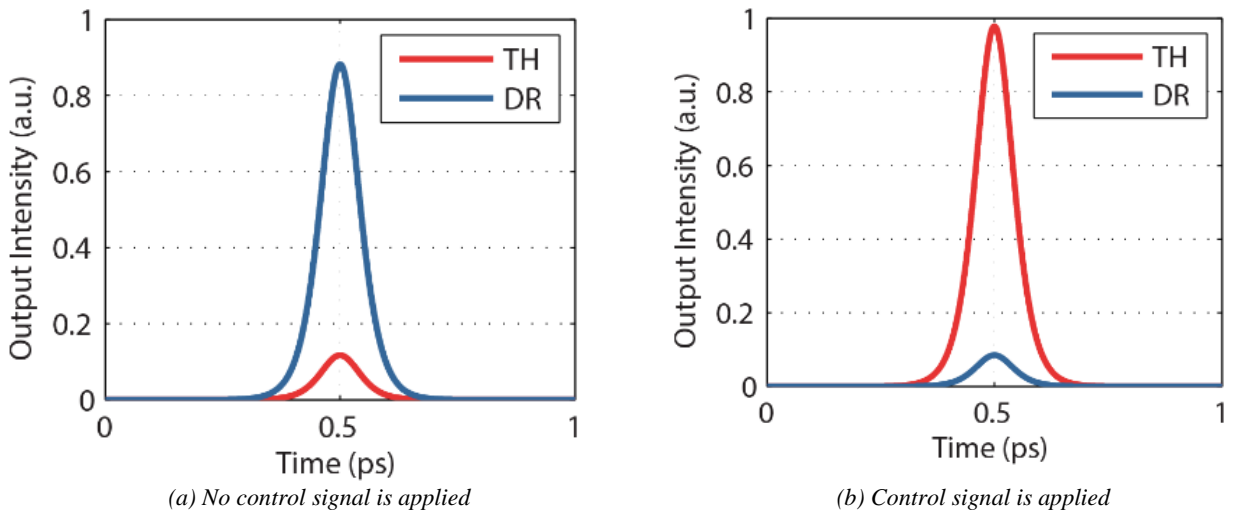
Parameter variables	Explanation	values
$R$	Radius of the ring waveguide (measured from the center of the ring to the center of the waveguide)	$1.55 \mu\text{m}$
$W$	Width of the waveguides	$\sim 290$ to $\sim 440 \text{ nm}$
$H$	Height of the waveguides	$250 \text{ nm}$
$L$	Circumference of the ring waveguide (optical path lengths in a ring)	$9.74 \mu\text{m}$
$A_{\text{eff}}$	Effective mode core area	$0.25 \mu\text{m}^2$
$\kappa$	Coupling coefficients	0.25
$\gamma$	Coupling loss	0.01
$\alpha$	Intensity attenuation loss inside the ring	$0.05 \text{ dBmm}^{-1}$
$n_{\text{eff}}$	Effective refractive index of the ring (InGaAsP/InP)	3.34
$\Delta n$	Change of refractive index when control is applied (Bright soliton)	$3.5 \times 10^{-3}$
$\lambda_R$	Resonance wavelength	$1.55 \mu\text{m}$
$\Delta\lambda_R$	Resonance wavelength after control is applied (Bright soliton)	$1.54 \mu\text{m}$



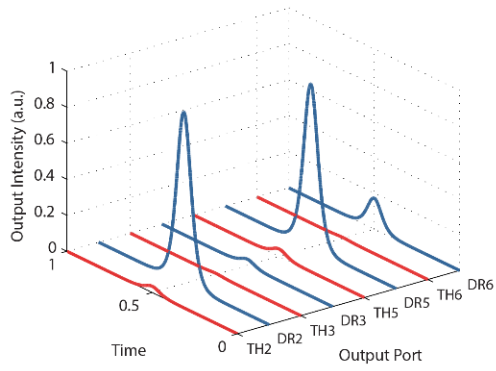
**Fig.3:** Transmission characteristics of bright soliton pulse within the MRR when the ring radius is  $1.55 \mu\text{m}$ ,  $\kappa=0.25$ ,  $m=21$  and  $\lambda_R=1.55 \mu\text{m}$ , where the dark-bright soliton pair is processed as the “On-Off” signals.



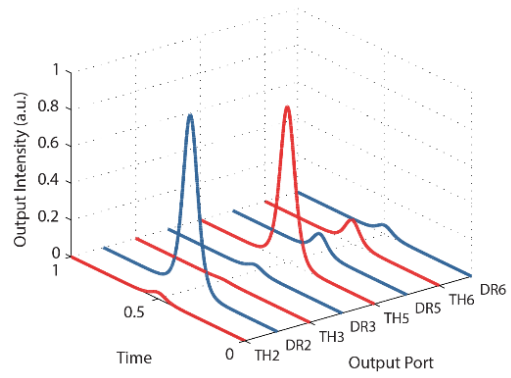
Fig. 5(d) shows the output when the input XYZ is “011”. This case is the same as the previous case for the first and second states where (XY=01), and the optical is transmitted to through-port (TH2) as optical logic “1”. The signal from TH2 is then used to be input signal of MRR2 via add-port and appear at the through-port (TH4) due to the resonance condition and applied to MRR6. Where in this state, the control input is applied (Z=0), thus, the optical signal is appeared at through-port (TH6) and represents the optical logic “1000010” at output-ports “TH2-DR2-TH3-DR3-TH5-DR5-TH6-DR6”. Fig. 5(e) shows the output when the input XYZ is “100”. This case, the control pulse is applied to MRR1 (X=1), thus the input signal is transmitted to through-port (TH1). Next, the signal from TH1 is input into MRR3 via input-port and control input (Y=1) is applied to add-ports (AD2), therefore, the optical signal is appeared at through-port (TH3) to be optical logic 1. The signal from TH3 is then used to be input signal of MRR4 via input-port and appear at the drop-port (DR4) due to the resonance condition. The signal is then inputted into MRR6. For this state, no control input (Z=0) is applied, thus, the optical signal is appeared at drop-port (DR6) and represents the optical logic “00010001” at output-ports “TH2-DR2-TH3-DR3-TH5-DR5-TH6-DR6”. Fig. 5(f) shows the output when the input XYZ is “101”. This case is the same as the previous case for the first and second states where (XY=10), and the optical signal is transmitted to drop-port (DR3) as optical logic “1”. Where in this state, the control input is applied (Z=1), thus, the optical signal from MRR4 is appeared at through-port (TH6) and represents the optical logic “1000010” at output-ports “TH2-DR2-TH3-DR3-TH5-DR5-TH6-DR6”. Fig. 5(g) shows the output when the input XYZ is “110”. This case, the control pulse is applied to MRR1 (X=1), thus the input signal is transmitted to through-port (TH1). Next, the control input (Y=1) is applied to MRR3, thus the signal from MRR1 (TH1) is through-port (TH3) to be optical logic 1. The signal from TH3 is again used as the input signal of MRR4 via input-port and appear at the drop-port (DR4). The signal is then transmitted into MRR5. For this state, no control input (Z=0) is applied, thus, the optical signal is appeared at drop-port (DR5) and represents the optical logic “00100100” at output-ports “TH2-DR2-TH3-DR3-TH5-DR5-TH6-DR6”. Lastly, Fig. 5(h) shows the output when the input XYZ is “111”. This case is the same as the previous case for the first and second states where (XY=11), and the optical signal is transmitted to through-port (TH3) as optical logic “1”. Where in this state, control input (Z=1) is applied to MRR5, thus, the optical signal from MRR4 (DR4) is appeared at through-port (TH5) and represents the optical logic “00101000” at output-ports “TH2-DR2-TH3-DR3-TH5-DR5-TH6-DR6”. In Table 3, we conclude the optical logic of all-optical ALU circuit obtained from output-ports TH2, DR2, TH3, DR3, TH5, DR5, TH6, DR6 of MRR2, MRR3, MRR5, MRR6, respectively. Where the output signal can be used to perform all-optical full-adder/half adder. The arithmetic operation can be done by using beam-splitter and beam combiner to split and combine optical output intensity such as SUM=TH5+DR6; CAR=TH3+TH6 for summation and carry out of full-addition, DIF=TH5+DR6; BOR=TH2+TH5 for difference and borrow of full-subtraction, respectively. This output logic can be implemented in other arithmetic and logic operation such as XOR gate, XNOR gate, increment and decrement.



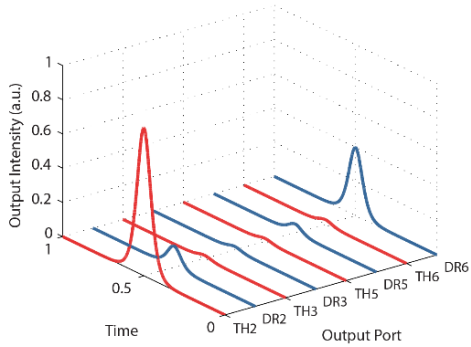
**Fig. 4:** Transmission signal at through-port (TH) and drop-port (DR) of MRR, when the peak output intensity represented to be logic “1” and the weak output intensity is represented to be logic “0”, the secure signal can be obtained by the applying the control input signal.



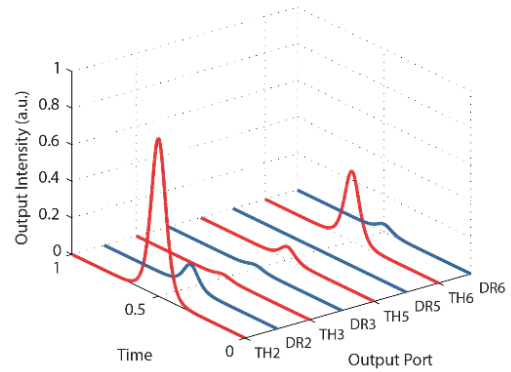
(a) output logic is "01000100"



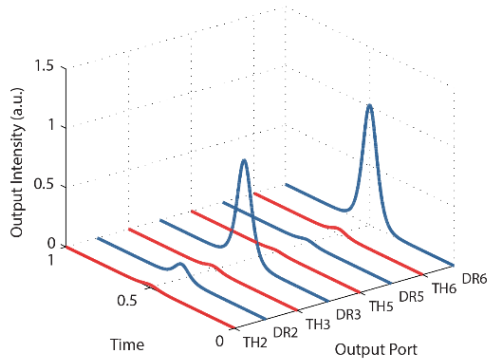
(b) output logic is "01001000"



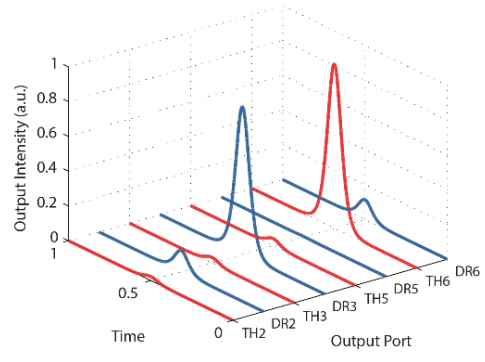
(c) output logic is "10000001"



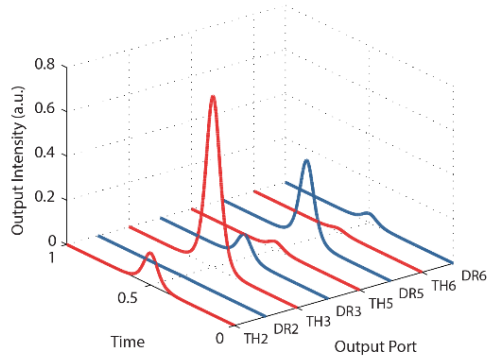
(d) output logic is "10000010"



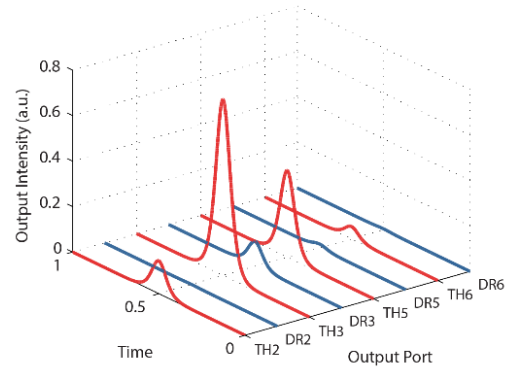
(e) output logic is "00010001"



(f) output logic is "00010010"



(g) output logic is "00100100"



(h) output logic is "00101000"

**Fig. 5:** Transmitted signals at output-ports of MRR2, MRR3, MRR5 and MRR6 when input logic "XYZ" is (a) "000", (b) "001", (c) "010", (d) "011", (e) "100", (f) "101", (g) "110", (h) "111"

**Table 3:** Conclusion of all-optical full-adder/subtractor

Inputs			Output Ports								Results			
X	Y	Z	TH2	DR2	TH3	DR3	TH5	DR5	TH6	DR6	CAR	BOR	SUM	DIF
<i>D</i>	<i>D</i>	<i>D</i>	<i>D</i>	<i>B</i>	<i>D</i>	<i>D</i>	<i>D</i>	<i>B</i>	<i>D</i>	<i>D</i>	<i>D</i>	<i>D</i>	<i>D</i>	<i>D</i>
<i>D</i>	<i>D</i>	<i>B</i>	<i>D</i>	<i>B</i>	<i>D</i>	<i>D</i>	<i>B</i>	<i>D</i>	<i>D</i>	<i>D</i>	<i>D</i>	<i>B</i>	<i>B</i>	<i>B</i>
<i>D</i>	<i>B</i>	<i>D</i>	<i>B</i>	<i>D</i>	<i>D</i>	<i>D</i>	<i>D</i>	<i>D</i>	<i>D</i>	<i>B</i>	<i>D</i>	<i>B</i>	<i>B</i>	<i>B</i>
<i>D</i>	<i>B</i>	<i>B</i>	<i>B</i>	<i>D</i>	<i>D</i>	<i>D</i>	<i>D</i>	<i>D</i>	<i>B</i>	<i>D</i>	<i>B</i>	<i>B</i>	<i>D</i>	<i>D</i>
<i>B</i>	<i>D</i>	<i>D</i>	<i>D</i>	<i>D</i>	<i>D</i>	<i>B</i>	<i>D</i>	<i>D</i>	<i>D</i>	<i>B</i>	<i>D</i>	<i>D</i>	<i>B</i>	<i>B</i>
<i>B</i>	<i>D</i>	<i>B</i>	<i>D</i>	<i>D</i>	<i>D</i>	<i>B</i>	<i>D</i>	<i>D</i>	<i>B</i>	<i>D</i>	<i>D</i>	<i>D</i>	<i>D</i>	<i>D</i>
<i>B</i>	<i>B</i>	<i>D</i>	<i>D</i>	<i>D</i>	<i>B</i>	<i>D</i>	<i>D</i>	<i>B</i>	<i>D</i>	<i>D</i>	<i>B</i>	<i>D</i>	<i>D</i>	<i>D</i>
<i>B</i>	<i>B</i>	<i>B</i>	<i>D</i>	<i>D</i>	<i>B</i>	<i>D</i>	<i>B</i>	<i>D</i>	<i>D</i>	<i>D</i>	<i>B</i>	<i>B</i>	<i>B</i>	<i>B</i>

Logic “0” is Dark soliton (*D*); logic “1” is Bright soliton (*B*).

## 5. Conclusion

We have proposed the design circuit of the ALU that can be used to perform the two arithmetic operations which are full-addition and full-subtraction using the semiconductor (*GaAsInP/P*) microring resonator circuits. By using the bright soliton input signal, the operation can be successfully achieved by dark-bright soliton conversion within microring resonator, which can be used to represent optical logic NOT gate (optical switching). This dark-bright soliton conversion can be controlled, where the high-security communication in long distance using such concept has been reported and confirmed [29, 30]. The simulation shows that the ultrafast-optical switching time of ( $\tau_{sw}=0.14$  ps), an on-off ratio of ~47.99 and propagation time of ~0.30 ps are obtained. This design circuit is also the small in physical size, which is flexible in order to demonstrate in the larger amount of bits processing and considering for experimentation and fabrication.

## Acknowledgement

One of the authors (S. Soysouvanh) would like to give an acknowledgement to AUN/SEED-Net for financial support in his PhD program.

## References

- [1] S. Kumar, S. Kumar Raghuvanshi, B. M. A. Rahman, "Design of universal shift register based on an electro-optic effect of LiNbO<sub>3</sub> in Mach-Zehnder interferometer for high-speed communication", *Opt Quant Electron*, 47, 3509, 2015.
- [2] Y. Tian, Y. Zhao, W. Chen, A. Guo, D. Li, G. Zhao, Z. Liu, H. Xiao, G. Liu, and J. Yang, "Electro-optic directed XOR logic circuits based on parallel-cascaded micro-ring resonators," *Opt. Express*, 23, 26342-26355, 2015.
- [3] A. Godbole, P. P. Dali, V. Janyani, T. Tanabe and G. Singh, "All optical scalable Logic gates using Si<sub>3</sub>N<sub>4</sub> microring resonators," *IEEE Journal of Selected Topics in Quantum Electronics*, 22(6), 326-333, 2016.
- [4] F. M.S. Mehdizadeh and H. Alipour-Banaei, "Proposal for 4-to-2 optical encoder based on photonic crystals," *IET Optoelectronics*, 11(1), 29-35, 2017.
- [5] S. K. Garai, "A novel all-optical frequency-encoded method to develop arithmetic and logic unit (ALU) using semiconductor optical amplifiers," *Lightwave Technology*, 29(23), 3506-3514, 2011.
- [6] D. K. Gayen, A. Bhattacharyya, T. Chattopadhyay and J. N. Roy, "Ultrafast all-optical half adder using quantum-dot semiconductor optical amplifier-based Mach-Zehnder interferometer," *J Lightwave Technology*, 30(21), 3387-3393, 2012.
- [7] T. Chattopadhyay, "Terahertz optical asymmetric demultiplexer (TOAD) based half-adder and using it to design all-optical flip-flop," *Optik - International Journal for Light and Electron Optics*. 123, 1961 – 1964 2012.
- [8] A.I., Stanley, E. James and F.U. Nweke, "The use of SOA-based Mach-Zehnder interferometer in designing/implementing all-optical integrated full adder-subtractor and demultiplexer", *Indian Journal of Engineering & Material Sciences*, 6 (1) , 40-44, 2015.
- [9] S. Kaur, R. Kaler, and T. Kamal, "All-optical binary full adder using logic operations based on the nonlinear properties of a semiconductor optical amplifier," *J. Opt. Soc. Korea*, 19, 222 – 227, 2015.
- [10] Theresal T., Sathish K., Aswinkumar R., "A new design of optical reversible adder and subtractor using MZI", *International Journal of Scientific and Research Publications*, 5(4), 1-6, 2015.
- [11] A. Raj, K. Bhambri and N. Gupta, Realization of all-optical full adder by utilizing DM soliton pulses. *International Journal of Computer Applications*, 96(19), 13-16, 2014.
- [12] I.S.Amiri, M.M.Ariannejad, M.Ghasemi, H.Ahmad, "Transmission performances of solitons in optical wired link", *Applied Computing and Informatics*, 13(1), 92-99, 2017.

- [13] S. Seifert and P. Runge, "Revised refractive index and absorption of  $\text{In}_{1-x}\text{Ga}_x\text{As}_{y1-y}\text{P}_{1-y}$  lattice-matched to InP in transparent and absorption IR-region," *Opt. Mater. Express*, 6, 629-639, 2016.
- [14] Q. Xu, D. Fattal, and R. Beausoleil, "Silicon microring resonators with 1.5- $\mu\text{m}$  radius," *Opt. Exp.*, 16, 4309-4315 2008.
- [15] S. Thongmee, P.P. Yupapin, "All optical half adder/subtractor using dark-bright soliton conversion control", *Procedia Engineering*, 8,217-222, 2011.
- [16] Abbas Madani, Hamidreza Azarina, Hamid Latifi, Design and fabrication of a polymer microring resonator with novel optical material at add/drop geometry using laser beam direct write lithography technique, *International Journal for Light and Electron Optics*, 124(14), 1746-1748, 2013.
- [17] Shubin Yan, Minghui Li, Liang Luo, Kezhen Ma, Chenyang Xue, Wendong Zhang, "Optimisation design of coupling region based on SOI microring resonator", *Micromachines*, 6(1), 2014, 151-159, 2014.
- [18] V. Donzella, A. Sherwali, J. Flueckiger, S. Grist, S. Fard, and L. Chrostowski, "Design and fabrication of SOI micro-ring resonators based on sub-wavelength grating waveguides," *Opt. Exp.*, 23, 4791-4803, 2015.
- [19] A. Kumar, "Application of micro-ring resonator as high speed optical gray code converter", *Opt. Quant. Electron.*, 48, 460, 2016.
- [20] Chat Teeka, Panuwat Chaiyachet, Preecha P. Yupapin, "Soliton collision management in a microring resonator system", *Physics Procedia*, 2(1), 67-73, 2009.
- [21] C. Teeka, M. A. Jalil, P. P. Yupapin and J. Ali, "Novel tunable dynamic tweezers using dark-bright soliton collision control in an optical add/drop filter," *IEEE Transactions on NanoBioscience*, 9(4), 258-262, 2010.
- [22] B. Dai, S. Shimizu, X. Wang and N. Wada, "Simultaneous all-optical half-adder and half-subtractor based on two semiconductor optical amplifiers," *IEEE Photonics Technology Letters*, 25(1), 91-93, 2013.
- [23] D. K. Gayen and T. Chattopadhyay, "Designing of optimized all-optical half adder circuit using single quantum-dot semiconductor optical amplifier assisted Mach-Zehnder interferometer," *J Lightwave Technology*, 31(12), 2029-2035, 2013.
- [24] Wang, Weiqiang, Chu, Sai T., Little, Brent E., Pasquazi, Alessia, Wang, Yishan, Wang, Leiran, Zhang, Wenfu, Wang, Lei, Hu, Xiaohong, Wang, Guoxi, Hu, Hui, Su, Yulong, Li, Feitao, Liu, Yuanshan, Zhao, Wei, "Dual-pump Kerr micro-cavity optical frequency comb with varying FSR spacing", *Scientific Reports*, 6, 28501, 2016.
- [25] J.K Rakshit, J.N. Roy & T. Chattopadhyay, "A theoretical study of all optical clocked D flip-flop using single microring resonator", *J Comput. Electron.*, 13, 278, 2014.
- [26] J.K. Rakshit a, T. Chattopadhyay b, J.N. Roy, "Design of ring resonator-based all-optical switch for logic and arithmetic operations – A theoretical study", *International Journal for Light and Electron Optics*, 124(23), 6048-6057, 2013.
- [27] S. Mookherjea and M. A. Schneider, "The nonlinear microring add-drop filter", *Opt. Exp.*, 16, 15130-15136, 2008.
- [28] I. K. Hwang, M. K. Kim and Y. H. Lee, "All-optical switching in InGaAsP-InP photonic crystal resonator coupled with microfiber," *IEEE Photonics Technology Letters*, 19(19), pp. 1535-1537, 2007.
- [29] I. S. Amiri, S. Babakhani, G. R. Vahedi, J. Ali, P. P. Yupapin, "Dark-bright Solitons conversion system for secured and long distance optical communication", *IOSR Journal of Applied Physics*, 2(1) (Sep-Oct. 2012), pp. 43-48, 2012.
- [30] Phatharaworamet, T., Teeka, C., Jomtarak, R., Mitatha, S. and Yupapin, P.P., "Random binary code generation using dark-bright soliton conversion control within a Panda-ring resonator", *J Lightwave Technol.*, 28(19), 2804-2809, 2010.